The Northern Hemisphere Polar Jet Stream and its Connection to the Seasonal Prediction Skill of Weather Regimes over Europe

Lara Hellmich[1,2], Panos Athanasiadis[3], Mikhail Dobrynin[4], André Düsterhus[1,5], Marc Rautenhaus[6] ,Paolo Ruggieri[3], and Johanna Baehr[1]

[1]Institute of Oceanography, CEN, Universität Hamburg, Germany
[2]Max Planck Institute for Meteorology, Hamburg, Germany
[3]Euro-Mediterranean Center on Climate Change (CMCC), Bologna, Italy
[4]Deutscher Wetterdienst (DWD), Hamburg, Germany
[5]ICARUS, Department of Geography , National University of Ireland, Maynooth, Ireland
[6]Regional Computing Centre, CEN, Universität Hamburg, Germany

Universität Hamburg
DER FORSCHUNG | DER LEHRE | DER BILDUNG

European Geosciences Union

Max-Planck-Institut für Meteorologie

International Max Planck Research School on Earth System Modelling

The Northern Hemisphere Polar Jet Stream and its Connection to the Seasonal Prediction Skill of Weather Regimes over Europe

<u>Motivation:</u> The frequency of extreme weather events, such as storms or cold spells, critically depends on the prevailing **weather regime** —> **seasonal predictability** of these regimes is important.

<u>Problem:</u> Currently, the ability of **seasonal prediction systems** to predict such weather regimes over Europe is limited (Fig. 1a).

<u>Approach:</u> **Weather regimes** and the location of the **northern hemisphere polar jet stream** interact with each other. Specific weather regimes are associated with a northern, central, or southern position of the jet stream (northern position: **Ridge Regime**, central position: **Zonal Regime** (NAO+), southern position: **Greenland Blocking** (NAO-)). We try to use the relationship between weather regimes and the location of the jet stream to improve seasonal winter forecasts over Europe. The high correlation between the location of the jet stream and the **NAO index**, which represents two distinct weather regimes (Fig. 1b), serves as motivation. Furthermore, the high correlation between the ERA-Interim reanalysis and the MR-30 ensemble for the location of the jet stream (Fig. 1c) shows higher potential for an **improved forecast** than the NAO index.

<u>Data:</u> We use a **seasonal prediction system** based on the Max-Planck-Institute Earth-System-Model (MPI-ESM) and investigate a 30-member ensemble started every November, as well as the global reanalysis ERA-Interim as an observational reference.

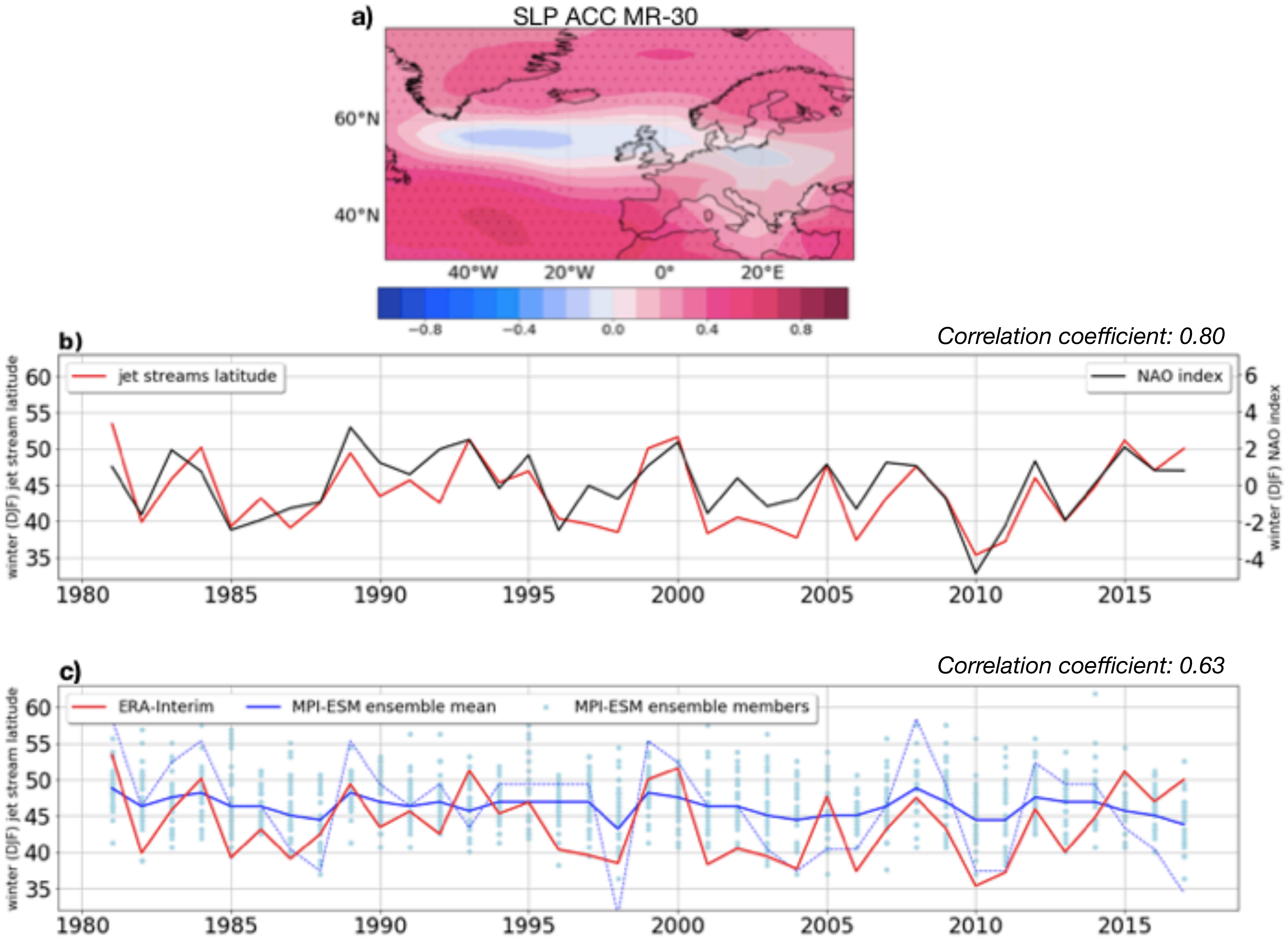

Fig. 1: Connection between the predictability of the jet streams latitude and the NAO index. a) Anomaly correlation plot as quantification of the prediction skill in the North Atlantic region for sea level pressure (SLP) in DJF. Shown are correlations between ERA-Interim and the MPI-ESM ensemble mean. b) Correlation between jet streams latitude and winter NAO index for the ERA-Interim reanalysis. c) Northern hemisphere winter polar jet streams latitude calculated from the maximum westerly wind speed over 900-700 hPa between 0° to 60°W for the ERA-Interim reanalysis (red line) and the MR-30 ensemble (blue line) and faint line showing the same time series after its variance has been adjusted to the observed variance (blue dotted line). Blue dots denote the MPI-ESM ensemble members.

Clustering of the Jet Stream Latitude

To quantify the jet stream, the northern hemisphere **5-day-running-mean zonal wind** is averaged over **900-700 hPa**. The jet stream's speed is defined as the maximum westerly wind speed, whereas the jet stream's latitude is defined as the **latitude of the maximum wind speed**. This method results in 99,900 polar jet stream lines, 30 for every winter day within our time period (37 years x 90 days per winter x 30 ensemble members).

To associate different jet stream latitudes with weather regimes, we classify our data through a **k-mean clustering**. For the jet stream positions the k-means clustering separates the given jet stream core lines into groups with similar jets stream latitudes and shapes. We then average the corresponding SLP anomaly fields of all winter days within each cluster group. With this method, it is possible to assign a specific pressure anomaly field to every cluster of jet stream positions. **The position of the jet stream allows us to draw conclusions about 3 dominant weather regimes.** This relationship can not only be found in the ERA-Interim, but also in the MR-30 ensemble (Fig. 2).

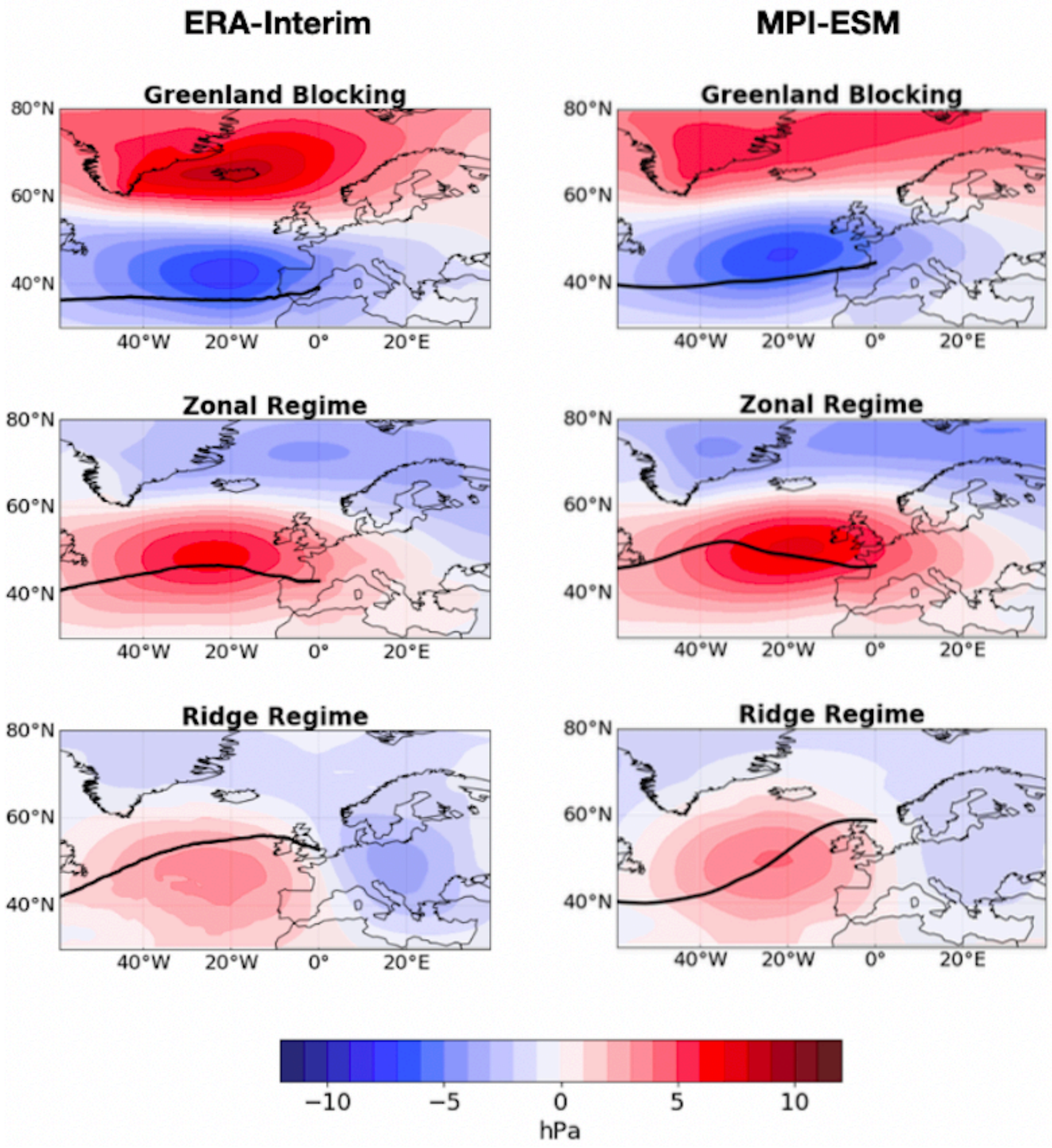

__Fig. 2:__ Northern hemisphere winter polar jet stream locations in DJF with the corresponding SLP- fields according to the jet streams location, for the ERA-Interim reanalysis (left column) and the MR-30 ensemble (right column). Clustered with k-means (k=4). Black lines show the mean jet stream position within a cluster. Red colors show positive anomalies in SLP, while blue colors show negative anomalies. The first row shows a southern position of the jet stream, associated with the Greenland Blocking, the second row shows a central position of the jet stream, associated with the Zonal Regime, and the third row shows a northern position of the jet stream associated with the Ridge Regime.

Comparison between ERA-Interim, the Ensemble Mean, and the Ensemble Selection

After we established that weather regimes can be determined from the location of the jet stream, the next step is to check how well the ensemble mean and ensemble selection agree with ERA-Interim.

We calculate the **two dominant regimes** (based on the number of days they occur each winter) in ERA-Interim and in the MR-30 ensemble mean without clustering the position of the jet stream. Furthermore, the two dominating clusters are shown for our selection method i.e. clustering the position of the jet stream and discarding the second NAO phase (this means the less dominant one).

Our selection of ensemble members leads to a much greater agreement with ERA-Interim than the MR-30 ensemble mean.

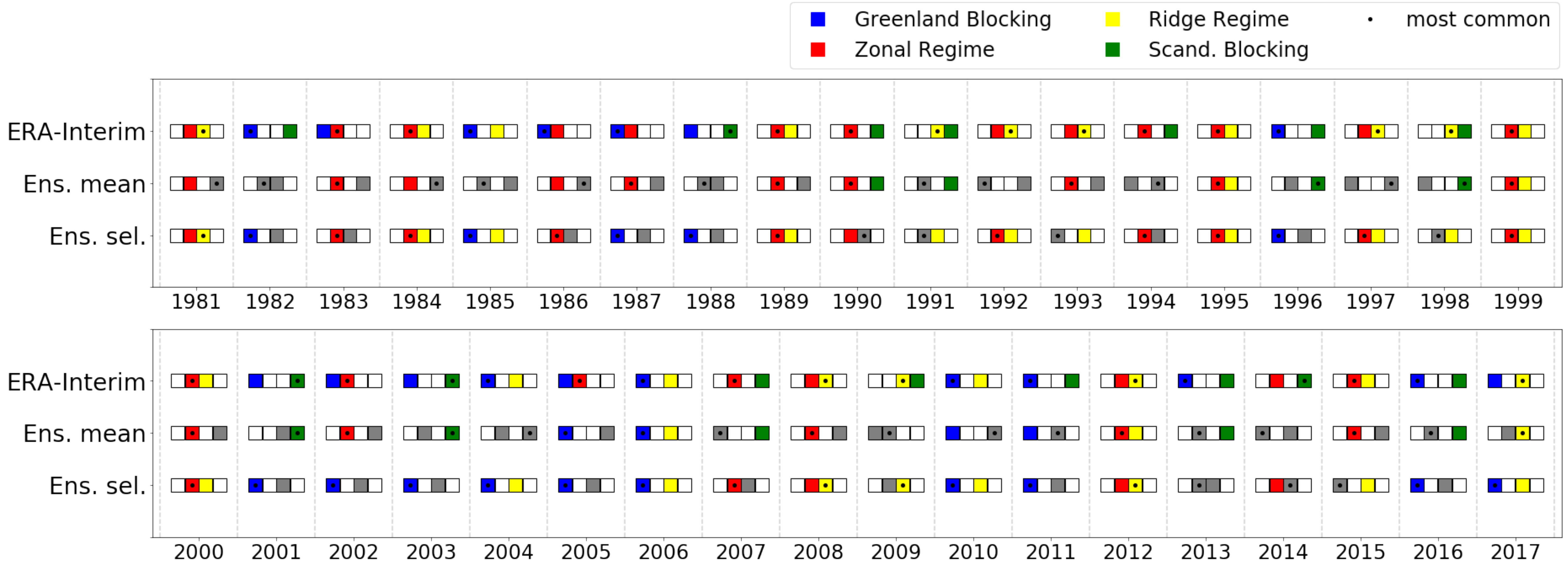

Fig. 3: *Two most dominant clusters per winter season in ERA-Interim (first row), the MR-30 ensemble mean without clustering, with an agreement of 44.60% on ERA-Interim, (second row) and the MR-30 ensemble with clustering and discarding the second NAO phase, with an agreement of 68.92% on ERA-Interim, (third row). Colored boxes mark regimes matching with ERA-Interim, while grey boxes mark differences. Dots within the different clusters mark the most dominant cluster.*

Prediction Skill of Different Common Regimes

Anomaly correlation coefficient (ACC) plots show how well the MR-30 ensemble SLP data match with the ERA-Interim reanalysis data in time and space. To quantify the prediction skill for SLP, we analyze ACCs between ERA-Interim and all ensemble members (Fig. 4a) and between ERA-Interim and different selections of the ensemble members (Fig. 4b-e).

Especially the most and second most common clusters per winter show **high correlations**, in some regions even higher than the ensemble mean. Furthermore, the third most common clusters per winter show a poor prediction skill.

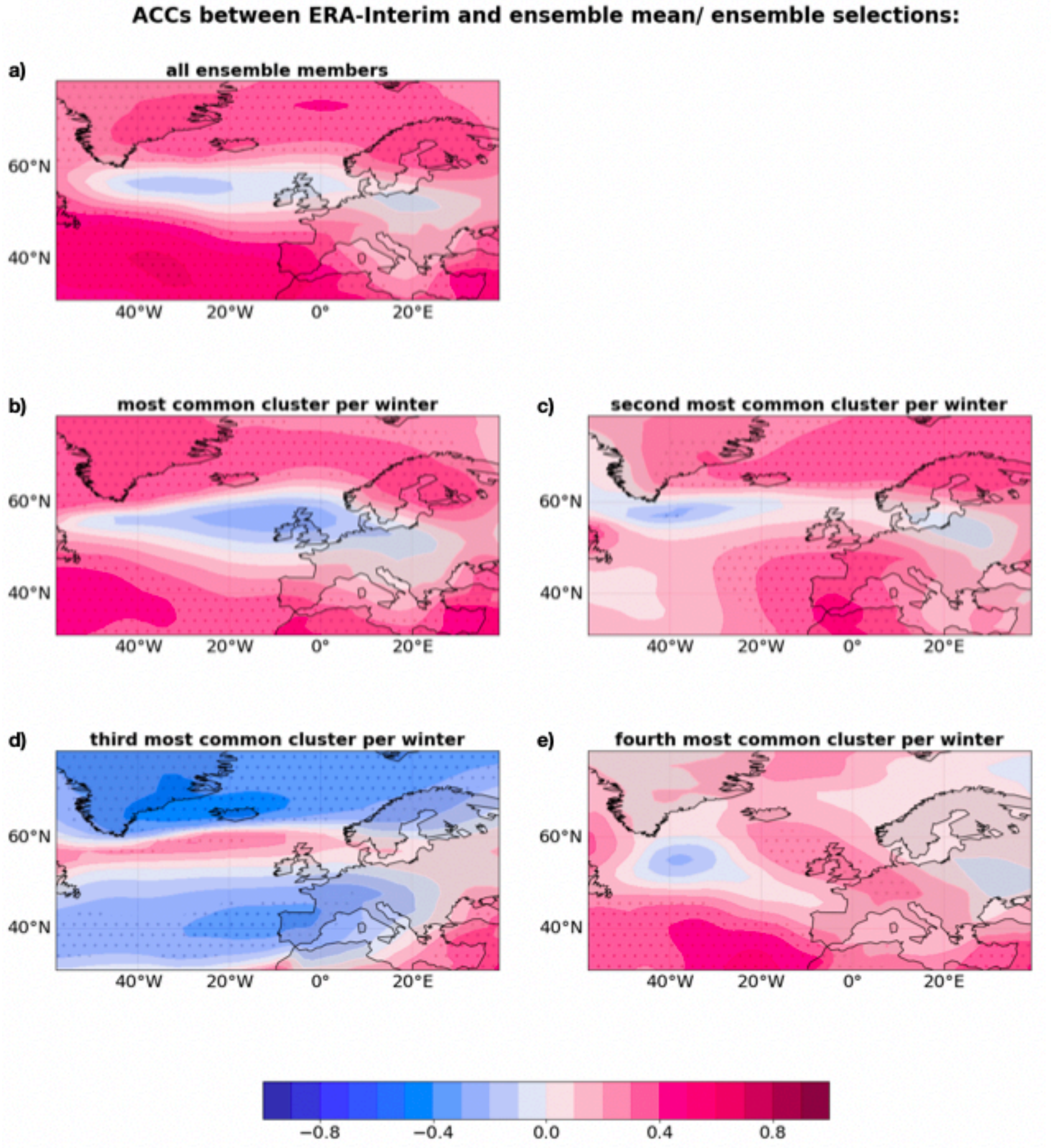

Fig. 4: *Anomaly correlation plot as quantification of the SLP prediction skill in the North Atlantic region in DJF. Shown are correlations between ERA-Interim and all MPI-ESM ensemble members (a), between ERA-Interim and a selection of ensemble members that show the most (b), second most (c), third most (d) and fourth most (e) common regime per winter. Dots represent significance at a 95% confidence level.*

Results and Conclusion

Based on the previous results, it seems reasonable to **combine the two most common clusters**. Again, anomaly correlations between ERA-Interim and our selection of ensemble members (as introduced before) due to clustering of the jet streams position (Fig. 5a), and between ERA-Interim and the same selection without the second NAO-phase (Fig. 5b) are shown. **Our selection of ensemble members leads to an increase in the prediction skill for SLP over the North Atlantic.**

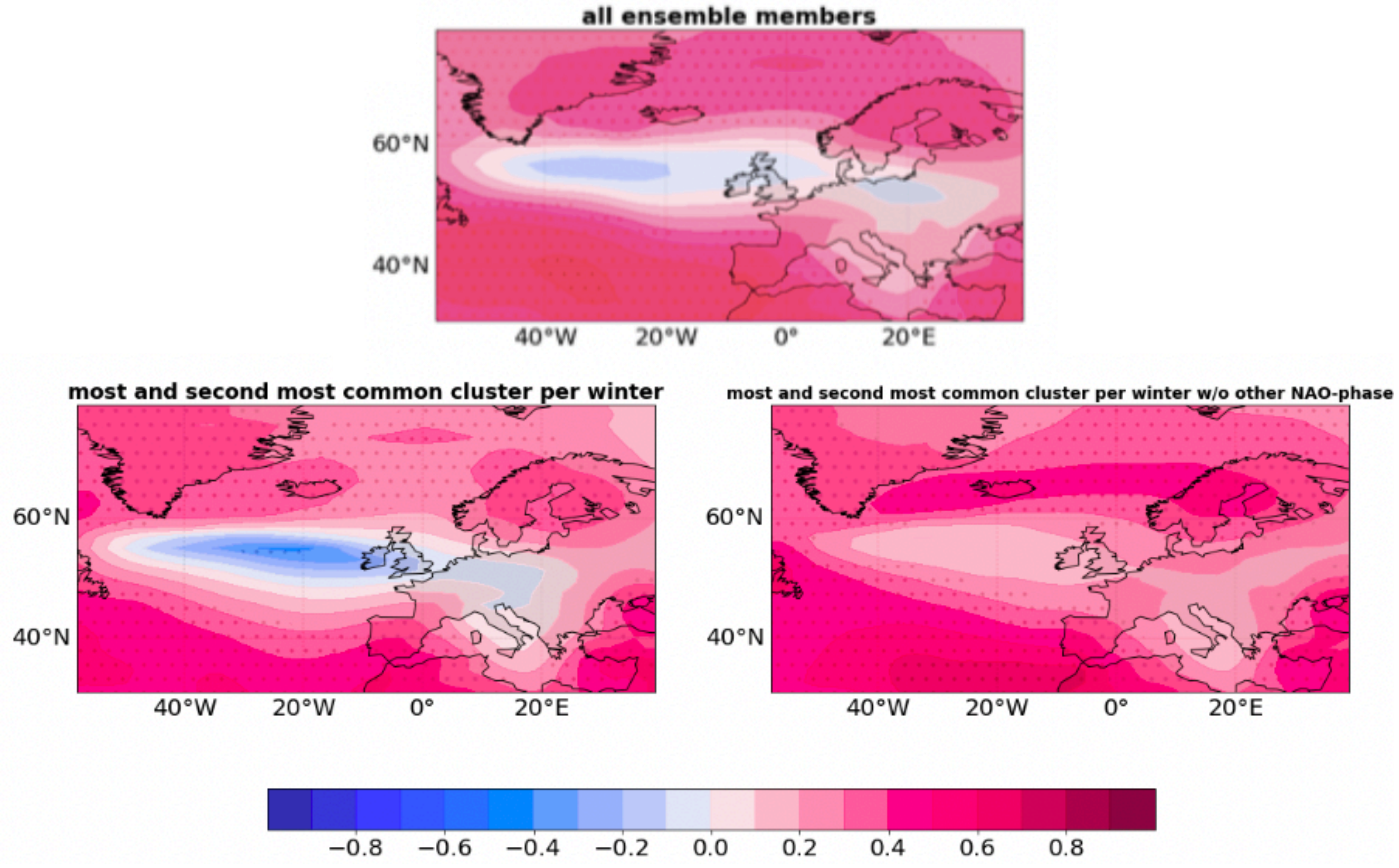

Fig. 5: Anomaly correlations between ERA-Interim and a combination of the two most common clusters with (a) and without (b) the other NAO-phase. Dots represent significance at a 95% confidence level.

Conclusion:

- **Our results show that complex phenomena such as weather regimes might be predictable on a seasonal scale for winter.**
- **Our MPI-ESM ensemble selection is able to represent the dominant weather regimes in almost all winters.**
- **By using a simple relationship, such as the location of the jet stream, we can improve the prediction skill for SLP.**

References

[Baehr et al. (2015)] J. Baehr, K. Fröhlich, M. Botzet, D. I. V. Domeisen, L. Kornblueh, D. Notz, R. Piontek, H. Pohlmann, S. Tietsche, W.A. Müller. (2015). The prediction of surfcae temperature in the new seasonal prediction system based on the MPI-ESM coupled climate model. Clim. Dyn., 44:2723-2735

[Berrisford et al. (2011)] P. Berrisford, D. Dee, P. Poli, R. Brugge, K. Fielding, M. Fuentes, P. Kållberg, S. Kobayashi, S. Uppala, and A. Simmons. (2011). The ERA- Interim archive. European Centre for Medium Range Weather Forecasts, ERA report series

[Cassou et al. (2003)] C. Cassou, L. Terray, J. W. Hurrell, and C. Deser. (2003). North Atlantic Winter Climate Regimes: Spartial Assymmetry, Stationarity with Time, and Oceanic Forcing. Journal of Climate, Volume 17

[Ghil and Roberston (2002)] Ghil M. and Roberston A.W. (2002). 'Waves' vs 'Particles' in the atmospheric phase space: a pathway to long-range forecasting?. Proc Natl Acad Sci USA, 99, 2493-2500

[Dee et al. (2011)] D. P. Dee, S. M. Uppala, A. J. Simmons, P. Berrisford, P. Poli, S. Kobayashi et al. (2011). The ERA-Interim reanalysis: configuration and perfor- mance of the data assimilation system. Q.J.R.Meteorol.Soc.137:553-597

[Dobrynin et al. (2018)] M. Dobrynin, D. I. V. Domeisen, W. A. Müller, L. Bell, S. Brune, F. Bunzel, A. Düsterhus, K. Fröhlich, H. Pohlmann, and J. Baehr. (2018). Improved Teleconnection-Based Dynamical Seasonal Predictions of Boreal Winter. Geophysi- cal Research Letters, Vol. 45, 3605-3614

[Giorgetta et al (2013)] Giorgetta, M. A., J. Jungclaus, C. H. Reick, S. Legutke, J. Bader, M. Boettinger, V. Brovkin, T. Crueger, M. Esch, K. Fieg, K. Glushak, V. Gayler, H.

[Grams et al. (2017)] C. M. Grams, R. Beerli, S. Pfenniger, I. Staffell, and H. Wernli. (2017). Balancing Europe's wind-power output through spatial deployment informed by weather regimes. Nature Climate Change. Volume 7.

[Neddermann et al. (2019)] N. C. Neddermann, W. A. Müller, M. Dobrynin, A. Düster- hus, and J. Baehr. (2019). Seasonal predictability of European summer climate re-assessed. Climate Dynamics, Volume 53, Issue 5-6, pp 3039-3056

[Madonna et al. (2017)] E. Madonna, C. Li, C. M. Grams, and T. Woolings. (2017). The link between eddy-driven jet variability and weather regimes in the North Atlantic- European sector. Q.J.R.Meteorol.Soc.143:2960-2972

[Kern et al. (2017)] M. Kern, T. Hewson, F. Sadlo, R. Westermann, and M. Raut- enhaus. (2017). Robust Detection and Visualization of Jet-stream Core lines in Atmospheric Flow. IEEE transactions on visualization and computer graphics no.10.1109/TVCG.2017.2743989, Vol. 24 (1) 893-902

[Parker et al. (2019)] T. Parker, T. Woollings, A. Weisheimer, C. O'Reilly, L. Baker, and L. Shaffrey. (2019). Seasonal Predictability of the Winter North Atlantic Oscilla- tion From a Jet Stream Perspective. Geophysical Research Letters, Vol. 46, 10,159- 10,167.

[Ruggieri et al. (2019)] P. Ruggieri, M. C. Alvarez-Castro, P. Athanasiadis, A. Bellucci, S. Materia, and S. Gualdi (2019). North Atlantic winter weather regimes and moist static transport by atmospheric transienteddies. 2019, Vol. 21, p1-1. 1p.

[Woollings et al. (2010)] T. Woollings, A. Hannachi and B. Hoskins. (2010). Variability of the North Atlantic eddy-driven Jet Stream. Q.J.R.Meteorol.Soc.136:856-868